Catalysis Today 176 (2011) 309–313

Contents lists available at ScienceDirect

Catalysis Today

journal homepage: www.elsevier.com/locate/cattod

Supported transition metal-oxide catalysts for HC-SCR DeNO$_x$ with propene

Denis Worch, Wladimir Suprun, Roger Gläser*

Institute of Chemical Technology, Universität Leipzig, Linnéstraße 3, 04103 Leipzig, Germany

ARTICLE INFO

Article history:
Received 2 September 2010
Received in revised form
30 November 2010
Accepted 2 December 2010
Available online 11 January 2011

Keywords:
DeNO$_x$
SCR
Hydrocarbon
Propene
Mixed-oxide catalyst

ABSTRACT

The selective catalytic reduction of nitrogen oxides by hydrocarbons (HC-SCR DeNO$_x$) on supported mixed-oxide catalysts is a promising technology for the treatment of exhaust gases from spark-ignition engines. In this work, the SCR of NO with propene on catalysts with Fe-, Cu-, V- and Ce-oxides supported on Al_2O_3, phosphated Al_2O_3 or SAPO-11, was investigated. As shown by their temperature-programmed reduction-profiles, the catalysts' behaviour for NO conversion depends mainly on the redox properties of the supported metal oxide. The acidic properties of these catalysts assessed by temperature-programmed reduction of ammonia can be neglected for NO$_x$ conversion. Catalysts prepared by sol–gel synthesis are more active for NO$_x$ conversion than catalysts prepared by wet impregnation. Probably, this is due to smaller metal oxide particles on the support surface in catalysts from sol–gel synthesis compared to those prepared by excess solution impregnation. Catalysts containing CuO$_x$ show highest NO conversion (at 350 °C), CeO$_x$- and FeO$_x$-containing catalysts show moderate NO conversion (at 350–450 °C), whereas VO$_x$- and FeO$_x$-containing catalysts favor total oxidation of propene already at low temperature.

1. Introduction

NO$_x$ are environmental pollutants that are made responsible, e.g., for the formation of ozone in the troposphere and the production of acid rain. The most promising method to reduce NO$_x$ under excess oxygen conditions is the selective catalytic reduction of NO$_x$ (SCR-DeNO$_x$). For instance, hydrocarbons [1], hydrogen [1], urea [2], ammonia [1], and oxygenates [3] were studied as reducing agents. In the presence of excess oxygen, a conventional three-way catalyst (TWC), which is commonly used for emission reduction in spark-ignition engines, is ineffective in reducing NO$_x$. That is why, *inter alia*, supported mixed-oxide catalysts have attracted much attention as potential candidates for the catalytic removal of NO$_x$ from lean-burn and diesel exhaust gases under excess oxygen conditions. Numerous works published over the last decade focused on investigations of SCR mechanism, the search for new catalysts and the use of different reducing agents. Of particular note are the works of the research group of Burch [1,4] for their pioneering research in investigating the detailed mechanism of HC-SCR over several catalysts such as Ag/Al_2O_3.

Recently, supported transition metal oxides were found to be highly active for NO$_x$ reduction by NH_3. The use of NH_3 causes high costs due to the necessary safety technology during transport and storage, damages by corrosion as well as the costs for the reducing agent itself. However, hydrocarbons and oxygenates are ingredients of off-gases. Lower hydrocarbons (C_1–C_4), higher hydrocarbons, gasoline, diesel fuel and alcohols (C_1–C_4) have all been investigated as reducing agents [1,5–7]. To develop more cost effective catalysts, supported transition metals or metal oxides of, e.g., Fe, Cu, Ce, Ni, V, Mn, may be used for catalytic NO$_x$ decomposition [8].

Up to date, many catalysts such as the zeolite Cu-ZSM-5 [9], Ag/Al_2O_3 [4], supported rare-earth oxides [10], La–Mn–Ba-perovskites [1] and supported noble metals [8] were studied for HC-SCR. Most of them are not active in the low-temperature region (<400 °C), except noble metal catalysts. The main requirement for HC-SCR catalysts is high catalytic activity in low temperature region (<400 °C). Most catalysts for HC-SCR DeNO$_x$ show high activity in higher temperature region (>400 °C), which is then also limited by the total oxidation of the reducing agent. Recently, Suprun et al. [11] investigated HC-SCR DeNO$_x$ in the presence of CH_4 over sulphated zirconium oxides doped with different metal oxides and found for the investigated mesoporous materials that catalytic activity increases with higher acid site density. These catalysts were mainly active in a temperature region of 400–500 °C. On the other hand, deactivation is a significant drawback, especially when real feeds are used, i.e., in the presence of water and/or SO_2 [12].

The goal of this work was to study the performance of Fe-, Cu-, V- and Ce-oxide supported on Al_2O_3, phosphated Al_2O_3 or SAPO-11 prepared by either sol–gel synthesis or excess solution impregnation, catalysts for HC-SCR of NO in the presence of propene and excess oxygen. Additionally, the role of the nature of the support and of added acidic components (phosphoric acid) on the catalytic activity and their resistance towards hydrothermal treatment were

* Corresponding author. Tel.: +49 3419736301.
E-mail address: roger.glaeser@chemie.uni-leipzig.de (R. Gläser).

0920-5861/$ – see front matter © 2011 Elsevier B.V. All rights reserved.
doi:10.1016/j.cattod.2010.12.008

Table 1
Physico-chemical properties (specific surface area A_{BET}, average pore diameter d_p, acid site density $n_{NH_3}/m_{cat.}$, metal loading wt.%) of mixed-oxide catalysts and support materials.

Catalyst	A_{BET} ($m^2\,g^{-1}$)	d_P (nm)	$n_{NH_3}/m_{cat.}$(mmol g^{-1})	Metal loading (wt.%)[a]
γ-Al_2O_3	257	12.4	187	n.a.[b]
FeO_x/Al_2O_3	220	9.4	146	8.7
VO_x/Al_2O_3	225	8.0	302	7.7
γ-Al_2O_3-PO_4	207	11.1	294	n.a.
FeO_x/Al_2O_3-PO_4	215	9.0	249	7.5
VO_x/Al_2O_3-PO_4	203	6.9	260	6.7
CuO_x/Al_2O_3-PO_4-SG	211	9.5	280	7.0
CuO_x/Al_2O_3–PO_4-I	157	11.9	302	3.6
CeO_x/Al_2O_3-PO_4-SG	153	5.3	170	6.5
CeO_x/Al_2O_3-PO_4-I	184	8.8	180	3.4
SAPO-11	113	0.6	2740	n.a.
$2CuO_x$/SAPO-11	64	n.d.[c]	2390	0.6
$6CuO_x$/SAPO-11	44	n.d.	2440	1.8
$12CuO_x$/SAPO-11	36	n.d.	2570	3.6
$2CeO_x$/SAPO-11	85	n.d.	2190	0.6
$6CeO_x$/SAPO-11	78	n.d.	1810	1.7
$12CeO_x$/SAPO-11	75	n.d.	1745	3.4

[a] Calculation based on synthesis composition.
[b] Not applicabel.
[c] Not determined.

studied. Investigations for the correlation between acid site density and NO conversion were also made. The stability towards SO_2 and H_2O as ingredients of the feed gas was not investigated.

2. Experimental

2.1. Catalyst preparation

Aluminium phosphate (Al_2O_3-PO_4, APO) was prepared by excess solution impregnating Al_2O_3 (Acros, specific surface area 256 $m^2\,g^{-1}$; mean pore diameter between 11.5 and 12.5 nm; AO) with H_3PO_4 (Acros, 85 wt.%). The support was used without further treatment. The impregnation with metal precursors was performed at 25 °C by contacting 10 g support with 25–50 cm^3 of an aqueous solution of the corresponding metal salts under constant stirring for 120 min. The molar relation between metal, alumina and phosphate was kept constant at $n_{Me}/n_{Al} = 1/10$ and $n_{PO_4}/n_{Al} = 1/12$. The following metal salts were used for impregnation: metal nitrates of Cu(II), Ce(III), Fe(II) (Fluka) and ammonium metavanadate (Aldrich). The impregnated MO_x/Al_2O_3-PO_4 were dried at 110 °C for 12 h and calcined in air for 4 h at 520 °C. Finally, the catalysts were pressed, sieved and the grain size fraction between 0.1 and 0.3 mm was used in the catalytic experiments. The MeO_x/SAPO-11 catalysts were also prepared by excess solution impregnation using Ce(III)- and Cu(II)nitrate with a ratio between metal and support of $n_{Me}/m_{SAPO\text{-}11}$ of 0.3, 1.0 and 1.9 mmol g^{-1}, respectively.

Cu- and Ce-containing MO_x/Al_2O_3-PO_4 catalysts were also prepared by sol–gel synthesis using the method proposed by Luna et al. [13]. The molar relation between metal, alumina and phosphate was kept equal as for catalysts prepared by the impregnation method. These catalysts were labelled as CuO_x/Al_2O_3-PO_4-I and CeO_x/Al_2O_3-PO_4-I (prepared by excess solution impregnation) and CuO_x/Al_2O_3-PO_4-SG and CeO_x/Al_2O_3-PO_4-SG (prepared by sol gel synthesis). The metal loadings of the prepared catalysts (wt.% metal) are given in Table 1.

2.2. Catalyst characterisation

The textural properties were determined from adsorption–desorption isotherms of nitrogen at −196 °C, using an ASAP 2010 apparatus (Micromeritics). The specific surface areas were determined by applying the BET equation at a relative pressure range $0.03 \le p/p \le 0.21$.

Powder X-ray diffraction (XRD) patterns were recorded on a Bruker D8 Advance X-ray diffractometer using a nickel-filtered Cu K_α (0.15418 nm) radiation source at 40 kV and 50 mA, respectively.

Temperature programmed desorption of ammonia (TPDA) was performed using a flow-type apparatus with a microreactor made from glass. The evolved gases were analyzed with a quadrupole mass spectrometer (Pfeiffer GSD 301). Prior to the analysis, the catalyst was pretreated in He (30 $cm^3\,min^{-1}$) at 250 °C for 1 h. After cooling to 95 °C, the samples were loaded with ammonia by consecutive pulses of 1 cm^3 ammonia until complete saturation of the surface was reached. After the removal of physisorbed ammonia by purging with helium, the sample was heated from 95 to 600 °C (heating ramp of 10 °C min^{-1}) in flowing He (50 $cm^3\,min^{-1}$) while analyzing the desorbed NH_3 by MS ($m/e = 16$). The amount of desorbed ammonia was quantified using a reference test, pulsing 1 cm^3 ammonia over 50 mg of inert quartz.

Temperature programmed reduction (TPR) profiles were obtained on an AMI 100 (Altamira) instrument equipped with a TCD. The catalysts were pre-treated in a flow of nitrogen (50 $cm^3\,min^{-1}$) at 300 °C for 30 min and then cooled down to room temperature. For the TPR measurements, a H_2/Ar mixture (5 vol.% H_2; 50 $cm^3\,min^{-1}$) was passed over the sample while heating from 30 to 800 °C (10 °C min^{-1}).

2.3. Catalytic conversion of NO with propene (HC-SCR DeNO$_x$)

Catalytic experiments were carried out using a continuous-flow apparatus with a fixed-bed reactor made from quartz. 0.2 g of catalyst and 0.2 g of α-Al_2O_3 as an inert material (particle size of 0.1–0.3 mm) were mixed and placed inside the reactor. Before the catalytic tests, the samples were heated up 400 °C and kept at this temperature for 1 h in flowing helium (100 $cm^3\,min^{-1}$). Subsequently, the temperature was lowered to 200 °C and the gaseous reactant feed consisting of 1100 ppm NO, 670 ppm C_3H_6, 4 vol.% O_2 in He as a carrier gas was led over the catalyst. The overall gas flow rate was 100 $cm^3\,min^{-1}$, corresponding to a gas hourly space velocity (GHSV) of 21,300 h^{-1}. The reaction temperature was increased in steps of 50 °C from 200 to 600 °C holding every temperature for 2 h. The concentrations of C_3H_6, CO_2, NO and NO_2 in the reactor effluent was continuously measured by an on-line FTIR-spectrometer (URAS-10, Hartmann & Braun). It was assured that, at each temperature, steady-state was achieved before the effluent gas was analyzed.

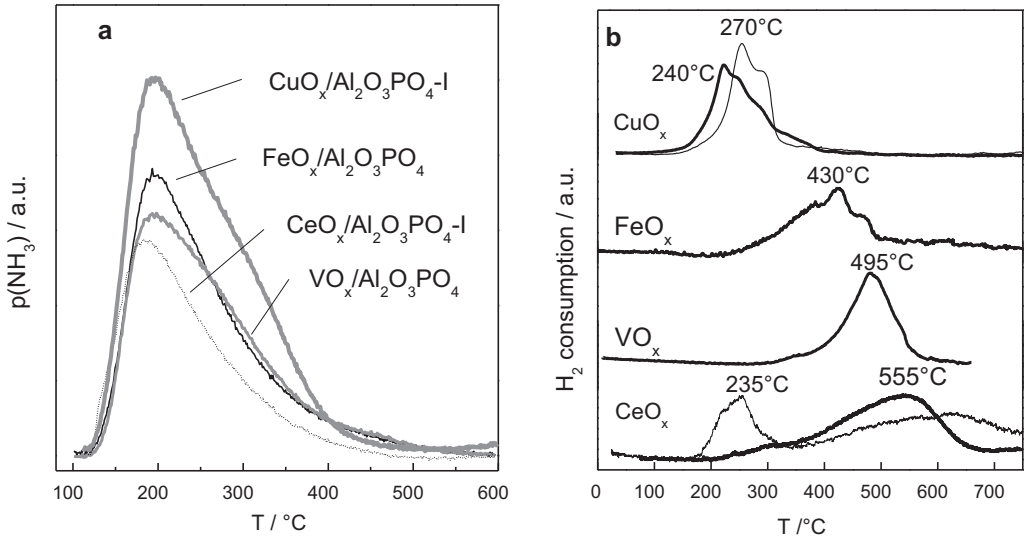

Fig. 1. TPDA- (a) and TPR- (b) profiles of MO_x/Al_2O_3-PO_4 catalysts. In graph (b), thick lines represent the catalysts prepared by excess solution impregnation and thin lines represent the catalysts prepared by sol–gel synthesis.

3. Results and discussion

3.1. Catalyst characterization

3.1.1. Textural properties

Table 1 shows the specific surface areas and the average pore size distribution of the investigated catalysts and support materials. Catalysts loaded with different metal oxides and phosphates clearly exhibit a lower specific surface area and pore diameter with respect to the unloaded supports. Please note, that the molar relation between metal, alumina and phosphate was kept constant at $n_{Me}/n_{Al} = 1/10$ and $n_{PO_4}/n_{Al} = 1/12$, respectively. The loss of specific surface area and pore diameter can be attributed to the deposition of the metal oxide particles. The reduction of specific surface area becomes more pronounced with increasing metal loading as shown for the Cu- and Ce-containing samples (Table 1). Note, however, that an apparent reduction of the specific surface area may also be caused by the increasing density of the samples due to the loading of the supports with metal. The presence of metal oxide particles is also confirmed by X-ray diffractograms (not shown). In the case of Ce-, Fe- and V-loaded samples, the diffractograms show sharp reflections of the corresponding metal oxides. For instance, reflections of the cubic phase CeO_2 and Ce_2O_3 ($2\theta = 27.6°$, 33.2°, 47.4° and 56.3° [14]) were detected on the samples CeO_x/Al_2O_3-PO_4 and $12CeO_x$/SAPO-11. Reflections typical for vanadium phosphate and V_2O_5 crystallites ($2\theta = 15.3°$, 20.4°, 26.3°, 31.1° and 34.4° [15,16]) were found for the VO_x/APO catalyst and reflections typical for Fe_2O_3, Fe_3O_4 [17] were observed for FeO_x/APO. These observations are in agreement with the results of Bautista et al. [13], reporting the formation of Fe- and V-oxides in MO_x/Al_2O_3-PO_4 composite materials. On the other hand, no reflections associated with crystalline metal oxide phases can be found in the case of the Cu modified samples as well as for $2CeO_x$- and $6CeO_x$/SAPO-11. This suggests that Cu- or Ce-oxides on these samples form very small particles beyond the detection limits of XRD or that they were incorporated into the amorphous framework of γ-Al_2O_3. [17].

3.1.2. Acidic and redox properties of the catalysts

In Fig. 1a, the TPDA profiles recorded for different metal oxides loaded by excess solution impregnation onto phosphated alumina (Al_2O_3-PO_4) are shown. For all samples, the TPDA profiles show a maximum at ca. 200 °C, corresponding to weakly bound ammonia. Evidently, the metal oxides do not affect the strength distribution of the acid sites on the samples surface. However, the Cu-containing sample exhibits the highest overall density of acid sites. The acid densities for the other samples prepared here are given in Table 1. For most of the catalysts, the acid site density supported on alumina and phosphated alumina decreases upon loading with the metal oxides indicating a blocking of the acid sites by the metal oxides. The catalysts with SAPO-11 as the support exhibit a much higher acid site density than the catalysts with the other two supports. There is also a decrease of the acid site density observed with increasing metal loading. In this case, the decrease of the acid site density is roughly proportional to the amount of loaded metal oxide.

Information about the redox properties of the metal oxide components is obtained from TPR profiles which are shown for the Cu-, Ce-, Fe- and V-containing catalysts on the Al_2O_3-PO_4 support in Fig. 1b. The reduction of copper oxide proceeds at relatively low temperatures between 160 and 350 °C with a maximum at 240 °C for the catalyst prepared by excess solution impregnation and at 270 °C with a significant shoulder at 310 °C for the catalyst prepared by sol–gel synthesis. The areas of these profiles are nearly equal. Assuming that only CuO is present on this catalyst, the amount of consumed hydrogen indicates that about 90% of CuO was reduced. In contrast, the Fe-, V- and Ce-based catalysts from impregnation are reduced at increasingly higher temperature with maxima at 430, 495 and 555 °C, respectively. The reduction of the CeO_x-containing catalyst prepared by sol–gel synthesis proceeds at considerably lower temperatures with a maximum at 235 °C and a sholder at 555 °C. The reduction of Ce^{4+} to Ce^{3+} species takes place in a temperature range of 250–550 °C and, in contrast the reduction of Ce^{3+} to Ce^0 (not shown in Fig. 1), proceeds at higher temperatures, i.e., in a range of 750–1050 °C [18]. The fact that the reduction of the Ce^{4+} species on CeO_x/Al_2O_3-PO_4-SG proceeds at lower temperature compared to those on CeO_x/Al_2O_3-PO_4-I suggests that this catalyst contains more Ce^{4+} species located at the surface. These species are, therefore, more easily reducible than those on the Ce-based catalyst prepared by excess solution impregnation. The reduction peaks of the Fe-, V- and Ce-based catalysts are tentatively attributed to FeO and Fe_2O_3, V_2O_5, CeO_2 and Ce_2O_3, respectively. Additionally, a small shoulder at around 350 °C is visible in the TPR profile of the VO_x/APO catalyst. According to a recent report of Liu [19], this low-

temperature reduction can be attributed to amorphous vanadium oxide well dispersed on the support surface.

3.2. Catalytic conversion of NO with propene

The maximum conversion of NO in the HC-SCR with propene over the catalysts studied here is summarized in Fig. 2a. Among all catalysts, the Cu-containing catalyst prepared by sol–gel synthesis and with phosphated alumina as the support showed the highest NO conversion of 33% which was achieved at 350 °C. Also for SAPO-11 as the support, the Cu-containing catalysts show the highest NO conversion. This might be related to facile reduction of the CuO_x species as supported by the TPR-profiles (see Fig. 1b). The V- and Fe-containing catalysts, except FeO_x/Al_2O_3, are highly active for propene conversion at low temperature, i.e., in the range of 250–300 °C. The maximum NO conversion observed on Ce-containing catalyst was 15.5% at 400 °C with SAPO-11 as support. Fig. 2b shows that the VO_x-containing catalysts exhibit high selectivity for N_2O (>90%). The other investigated catalysts show a moderate N_2O selectivity in the range of 20–40% with the exception of CuO_x/Al_2O_3-PO_4-SG and $2CeO_x$/SAPO-11, the N_2O selectivity of which is below 10%.

As shown in Fig. 3a, the catalytic activity depends also on the preparation method. As discussed in Section 3.1.1 above, the catalysts prepared by sol–gel synthesis contain smaller metal oxide particles on the support surface than the catalysts prepared by excess solution impregnation. This results in a higher activity for the reduction of NO [17]. However, there is no clear influence of the particle size of the metal oxide on the propene conversion as can be observed from Fig. 3b.

A comparison of the NO and C_3H_6 conversion over the catalysts prepared by excess solution impregnation with phosphated alumina as the support is shown in Fig. 3c and d. The conversion of NO at a temperature of 350 °C decreases in the order: $CuO_x/APO > FeO_x/APO > CeO_x/APO \sim VO_x/APO$. At the same temperature, the conversion of propene on these catalysts decreases in the order: $CeO_x/APO > FeO_x/APO \sim CuO_x/APO > VO_x/APO$. The comparison of the order of NO conversion at 350 °C on these catalysts with their TPR-profiles (Fig. 1b) suggests that a lower reducibility

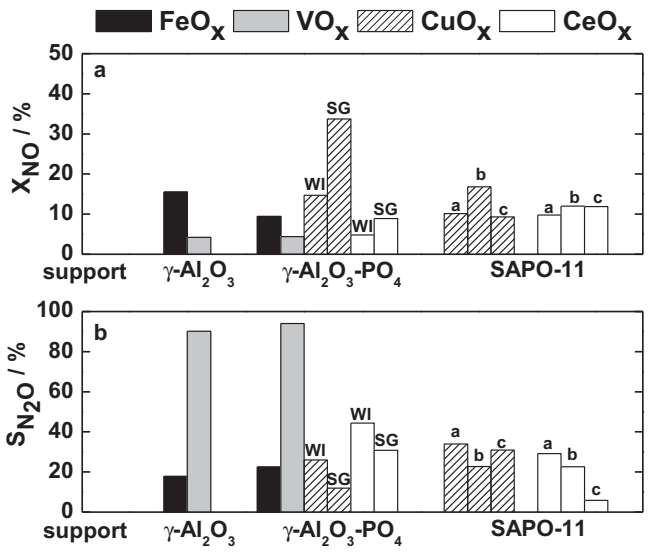

Fig. 2. Maximal NO conversion (a) and selectivity to form N_2O at maximal NO conversion (b) over supported mixed-oxide catalysts in the temperature range 350–400 °C. Reaction conditions: 1100 ppm NO, 670 ppm C_3H_6, 4 vol.% O_2 in He (carrier gas) at a total flow rate of 100 $cm^3\,min^{-1}$, $W/F = 0.12\,g\,s\,cm^{-3}$ (GHSV = 21,300 h^{-1}). $m_{cat.}$ = 200 mg diluted with 200 mg α-Al_2O_3. WI: excess solution impregnation; SG: sol–gel synthesis; *a*, *b*, *c*: $n_M/(n_M + n_{Al}) = 2$, 6, 12%.

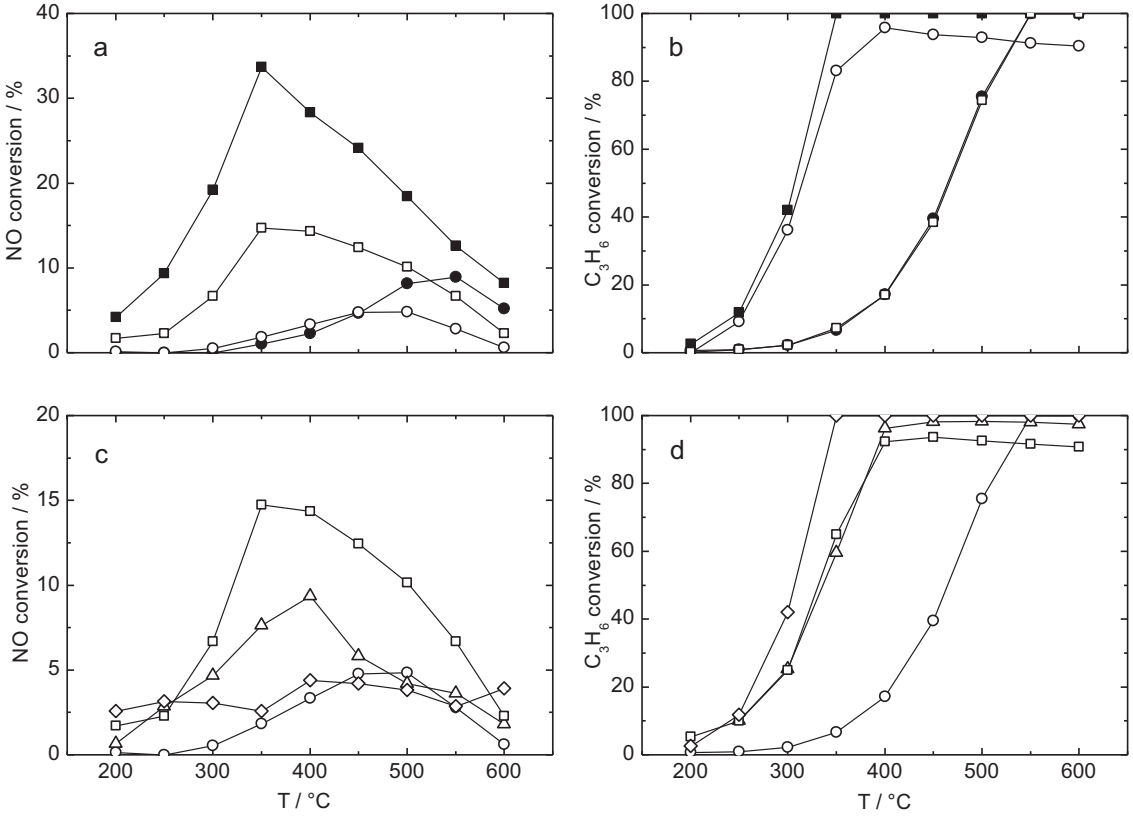

Fig. 3. NO conversion (a and c) and propene conversion (b and d) for the SCR of NO_x by C_3H_6 over (□) CuO_x/Al_2O_3-PO_4, (△) FeO_x/Al_2O_3-PO_4, (◊) VO_x/Al_2O_3-PO_4, (○) CeO_x/Al_2O_3-PO_4 catalysts prepared by sol–gel synthesis (full symbols) or excess solution impregnation (empty symbols). Reaction conditions as in Fig. 2.

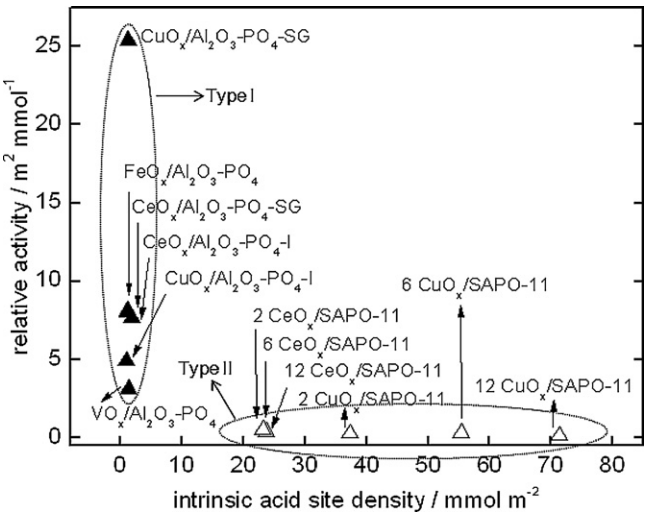

Fig. 4. Relative activity "RA" (RA = X_{NO}/intrinsic acid site density) as a function of intrinsic acid site density of SAPO-11 and Al_2O_3-PO_4 supported metal oxide catalysts.

of metal oxide species promotes a higher NO conversion. Further tests for hydrothermal stability (not shown) were carried out by temperature-programmed reaction from 200 to 600 and back to 200 °C (10 °C min^{-1}) with the same feed gas concentration as in the catalytic tests. However, no notable change of NO conversion was observed for all catalysts studied.

In contrast, however, no obvious correlation between the conversion of NO and the acid site density can be found for catalysts with SAPO-11 and Al_2O_3-PO_4 as supports (see Fig. 4). For selection of different parameters, which influence the catalysts performance, the parameter "relative activity (RA)" RA = X_{NO}/intrinsic acid site density was introduced. The influence of acid site density on the NO conversion can be explained with RA. As shown by Suprun et al. [11] for mesoporous materials, the activity increases with the acid site density. The SAPO-11 samples, marked as Type II in Fig. 4, have different acid site densities. But with higher acid site density, there is no noteworthy increase of relative activity. This fact can be explained by a limitation of the conversion by diffusion within the pores of SAPO-11. As for the catalysts supported on Al_2O_3-PO_4 or Al_2O_3 (Table 1), the effective pore diameter in SAPO-11 can be expected to decrease after loading with Cu- and Ce-oxides. For the catalysts with Al_2O_3-PO_4, marked as Type I in Fig. 4, and Al_2O_3 (not shown) as supports, the intrinsic acid site density is nearly the same, but different relative activities are observed. In this context, the type of metal oxide and also the synthesis method determine the activity of HC-SCR $DeNO_x$.

4. Conclusions

The promoting effect of supported transitions metal oxides supported on alumina, phosphated alumina and the silicoaluminophosphate SAPO-11 was investigated for the selective catalytic reduction of NO by propene in an oxygen-rich atmosphere. Among Ce-, V-, Cu- and Fe-oxides, a CuO_x/Al_2O_3-PO_4 catalyst showed the highest NO conversion. CuO_x/Al_2O_3-PO_4 prepared by the sol–gel method exhibits an activity with the highest NO conversion of 30–35% in the temperature range of 350–400 °C. The activity of CeO_x- and CuO_x/Al_2O_3-PO_4 catalysts is low, probably due to larger metal oxide particles on the support which favor the total oxidation of propene. However, NO-conversion on VO_x/Al_2O_3-PO_4 and VO_x/Al_2O_3 catalysts at 250–350 °C was lower than 10%. Generally, the presence of vanadia and iron oxide on the Al_2O_3-PO_4 support favors propene oxidation which, in turn, decreases the catalytic activity for NO reduction. VO_x-containing catalysts also show highest selectivity for N_2O, whereas the CuO_x/Al_2O_3-PO_4-SG and $2CeO_x$/SAPO-11 catalysts show lowest N_2O selectivity.

The difference in the SCR-$DeNO_x$ activity of Cu-, Ce-, V- and Fe-containing catalysts from impregnation can partly be attributed to their different redox properties. The lower SCR-$DeNO_x$ activity of microporous CuO_x/SAPO-11 catalysts compared to mesoporous CuO_x/Al_2O_3-PO_4 catalyst can be explained by pore diffusion effects. For mesoporous catalysts with Al_2O_3 or Al_2O_3-PO_4 as supports, the HC-SCR $DeNO_x$ is not diffusion controlled. Further investigations with SAPO-11 containing catalysts for diffusion controlled reactions are in progress. The acid site density of the investigated catalysts can be neglected for the HC-SCR $DeNO_x$ activity. Nevertheless, NO conversions above 35% were not yet reached. Thus, the search for more active catalysts for the HC-SCR $DeNO_x$ remains to be an important challenge in the field of environmental catalysis.

References

[1] R. Burch, Catal. Rev. 46 (2004) 271.
[2] A. Grossale, I. Nova, E. Tronconi, D. Chatterjee, M. Weibel, Top. Catal. 52 (2009) 1837.
[3] Y. Yu, H. He, Q. Feng, H. Gao, X. Yang, Appl. Catal. B 49 (2004) 159.
[4] R. Burch, J.P. Breen, F.C. Meunier, Appl. Catal. B 39 (2002) 283.
[5] K.I. Shimizu, A. Satsuma, Phys. Chem. Chem. Phys. 8 (2006) 2677.
[6] H. He, X. Zhang, Q. Wu, C. Zhang, Y. Yu, Catal. Surv. Asia 12 (2008) 38.
[7] S. Roy, M.S. Hedge, G. Madras, Appl. Energy 86 (2009) 2283.
[8] Z. Liu, S.J. Woo, Catal. Rev. 48 (2006) 43.
[9] A.E. Palomares, A. Uzcategui, A. Corma, Catal. Today 137 (2008) 261.
[10] L.L. Qu, J.J. Li, Z.P. Hao, L.D. Li, Catal. Lett. 131 (2009) 656.
[11] W. Suprun, K. Schaedlich, H. Papp, Chem. Eng. Technol. 28 (2005) 199.
[12] J.Y. Yan, G.D. Lei, W.H.M. Sachtler, H.H. Kung, J. Catal. 161 (1996) 43.
[13] F.M. Bautista, J.M. Campelo, A. García, D. Luna, J.M. Marinas, R.A. Quirós, A.A. Romer, Appl. Catal. A 243 (2003) 93.
[14] G.D. Angel, J.M. Padilla, I. Cuauhtémoc, J. Navarette, J. Mol. Catal. A: Chem. 281 (2008) 173.
[15] E.P. Reddy, R.S. Varma, J. Catal. 221 (2004) 93.
[16] X.H. Taufiq-Yap, Y.C.K. Goh, G.J. Hutchings, N.B. Dummer, Catal. Lett. 130 (2009) 327.
[17] W.M. Shaheen, K.S. Hong, Thermochim. Acta 381 (2002) 153.
[18] R. Rao, B.G. Mishra, Bull. Catal. Soc. India 2 (2003) 122.
[19] Z. Liu, Chem. Eng. Res. Des. 86 (2008) 932.